

## Supplementary Materials for

### Biosynthesis of monoterpene scent compounds in roses

Jean-Louis Magnard, Aymeric Roccia, Jean-Claude Caillard, Philippe Vergne, Pulu Sun, Romain Hecquet, Annick Dubois, Laurence Hibrand-Saint Oyant, Frédéric Jullien, Florence Nicolè, Olivier Raymond, Stéphanie Huguet, Raymonde Baltenweck, Sophie Meyer, Patricia Claudel, Julien Jeauffre, Michel Rohmer, Fabrice Foucher, Philippe Hugueney,\* Mohammed Bendahmane,\* Sylvie Baudino\*

\*Corresponding author. E-mail: sylvie.baudino@univ-st-etienne.fr (S.B.); philippe.hugueney@colmar.inra.fr (P.H.); mohammed.bendahmane@ens-lyon.fr (M.B.)

Published 3 July 2015, *Science* **349**, 81 (2015)  
DOI: 10.1126/science.aab0696

#### This PDF file includes:

Materials and Methods  
Figs. S1 to S13  
Tables S1 to S5  
Full Reference List

**Other Supplementary Material for this manuscript includes the following:**  
(available at [www.sciencemag.org/content/349/6243/81/suppl/DC1](http://www.sciencemag.org/content/349/6243/81/suppl/DC1))

Data S1 to S3 as Excel files

## **Materials and Methods**

### Plant materiel

Rose plants were field grown in five locations: at Saint-Etienne University, at Ecole Normale Supérieure, Lyon, at INRA Angers, at Lyon's Botanical Garden and at Meilland Richardier production fields in Heyrieux, France. Transgenic *Rosa chinensis* cv. 'Old Blush' plants were grown under controlled greenhouse conditions at Ecole Normale Supérieure, Lyon. Flower development was defined according to (16). Fragrant and non-fragrant rose varieties used for the correlation study were chosen in different cultivated rose families in order to maximize the diversity of this sample set. Selected varieties include very ancient cultivars such as *Rosa chinensis* cv. 'Old Blush' and 'Mutabilis', 'Alister Stella Grey' and more recent hybrids from various origins.

### RNA preparation, cDNA-AFLP-DD, gene expression analyses and CAPS marker design

Total RNA preparation, cDNA synthesis and the microarray experiment were performed as previously described (27). For cDNA-AFLP-DD experiment, PolyA<sup>+</sup> RNA was purified starting from total RNA (100 µg) using the Straight'As mRNA system kit (Novagen) according to manufacturer instructions. cDNA-AFLP-DD was performed with the displayPROFILE™ kit (Q Biogene) according to manufacturer instructions: polyA<sup>+</sup> RNA (1 µg) was used for double strand cDNA synthesis, the resulting cDNA were digested with the restriction enzyme *Taq1*, linked to adaptors and finally amplified by PCR. The amplicons were resolved on a sequencing polyacrylamide gel. Following autoradiography, candidate bands corresponding to differentially expressed products of interest were cut out from the gel. DNA was extracted from these polyacrylamide pieces by boiling 15 min in 10 mM Tris pH 8, 0.2 mM EDTA. Purified DNA was amplified using the adaptor primers ATGAGTCCTGACCGA and ACTGGTCTCGTAGACTGCGTACCCGA, cloned into the pGEMTeasy vector (Promega) and then sequenced.

Real time quantitative RT-PCR (qPCR) was performed with the FastStart Universal SYBR Green Master (Rox) (Roche Diagnostics GmbH, Mannheim, Germany) using the StepOnePlus real-time PCR system (Applied Biosystems). Reactions were run in duplicate and quantified against a relative standard curve made from a serially diluted stock cDNA containing the target sequence. Data collection and analysis were performed using the StepOne Software v2.1 (Applied Biosystems). Relative quantification of candidate genes was performed using rose orthologs of α-TUBULIN (*RhTUB*, Genbank accession number EC587914) and EF1-a (*RhEF1-a*, Genbank accession number BQ104256) as calibrators according to (28). Geometric means of the arbitrary units of the calibrator's transcripts were used to normalize the relative amount of candidate gene transcripts. Primers specific to each cDNA were used for expression analysis by qPCR.

After sequencing *RhNUDX1* in *Rosa chinensis* cv. 'Old Blush' (OB) and *Rosa x wichurana* (RW), SNP2CAPS software (29) were used to develop the CAPS markers (primers RhNudX\_F [GGGAAACGAGACAGTAGTAGTGG] and RhNudX\_R [GGGTTAAATCCATCCTGAACCAC], and *PstI* restriction enzyme). PCR reactions were carried out in 15 µl with GoTaq® Flexi DNA Polymerase according to the manufacturer's recommendations (Promega) under the following conditions: 95°C, 3 min; 35 X [95°C, 30 s; annealing temperature, 30 s; 72°C, 40 s]; 72°C, 5 min. PCR product (607bp) was digested with *PstI* (New England Biolabs). For the *RhNUDX1*

CAPS marker, RW is homozygous and present only the *b* allele which is non digested (607bp) whereas OB is heterozygous with the *a* (digested allele: 237bp and 370bp) and *b* (non digested: 607bp) alleles.

#### QTL and mapping analyses

JoinMap 4.0 (30) was used for the construction of the linkage map. SSR used for the map construction are described in (31) and (32). QTL analysis was carried out using MAPQTL® (33) and the OB female map. A LOD threshold at which a QTL was declared significant was determined according to a genome-wide error rate of 0.05 over 1000 permutations (34). Interval Mapping analysis was performed with a step size of 1cM to find regions with potential QTL effects i.e., where the LOD score was greater than the threshold and the percentage explained by the QTL ( $r^2$ ) was also presented.

#### Transient expression and subcellular localization of *RhNUDX1* in tobacco plants

For transient expression experiments, the *RhNUDX1* and the geraniol synthase coding sequences were cloned in the expression vector pMDC32 and then transformed into the *A. tumefaciens* strain C58 (pMP90). The GES cDNA was cloned either as a full-length form encoding the GES precursor, or as a truncated form encoding the mature GES protein according to (9). Agrobacteria cultures were then used to infiltrate leaves of *N. benthamiana* according to (35).

For subcellular localization, the *RhNUDX1* coding sequence was cloned in the expression vectors pMDC45 (2x35S-GFP-RhNUDX1) and pMDC83 (2x35S-RhNUDX1-GFP) (36) and then transformed as described above. C58 (pMP90) transformed with 2x35S-GFP in pBin19 were infiltrated in the same experiment as a control for cytosolic localization. Five days after infiltration, infiltrated leaf sectors were observed under a confocal microscope. Confocal micrographs were taken under TCS-SP2 inverted confocal scanning laser microscope (Leica Microsystems) with a x40/0.80W lens. The argon laser was set at 488 nm for GFP excitation and the helium-neon laser at 633 nm for chlorophyll. The fluorescent signals were captured through narrow bands: 500 to 550 nm for GFP, and 640 to 740 nm for chlorophyll.

#### Production of roses knockdown for *RhNUDX1*

A DNA fragment corresponding to part of the ORF of *RhNUDX1* (from bp 211 to bp 450, outside of the Nudix domain) was amplified and cloned in the vector pDONR207 for Gateway cloning. It was then cloned into the vector pK7GWIWG2 (II) (37) after the CaMV 35S constitutive promoter. The resulting construct, referred to as *p35S::RNAi-RhNUDX1*, was used to transform *Rosa chinensis* cv. ‘Old Blush’ (OB). RhNUDX1 sequence from OB and PM share 96% identity. Transgenic roses were produced according to (38). Plants transformed with the GUS reporter gene under the control of the 35S promoter (38), were used as a control (35S:GUS plants). Transgenic plants, referred to as *RNAi-RhNUDX1*, were characterized by qPCR. For metabolomic analyses, several cuttings of the same transgenic event were used.

For transient transformation assays, petals of the cultivar *R. x hybrida* cv. ‘The Mac Cartney rose’ were infiltrated with *p35S::RNAi-RhNUDX1* with the same protocol as the one used for *N. benthamiana*, except that no p19 construct was used. Petals were analyzed for their content in scent compounds 5 days after infiltration. As a control, C58 (pMP90) transformed with 2x35S-GFP in pBin19 were infiltrated in the same experiment. Three independent experiments were performed. One of these

experiments is presented in Fig. S5 and Table S4. For each experiment, 18 petals were infiltrated and analyzed individually (6 petals for each experimental condition).

#### Production of RhNUDX1 in *E. coli*, antibody preparation and Western-blot analyses

For antibody production and enzyme characterization, *RhNUDX1* coding sequence was cloned into the expression vectors pHXGWA and pHNGWA (39) to allow production of RhNUDX1 fused to a 6xHis-tagged thioredoxin or NusA proteins. A thrombin protease cleavage site was inserted between the thioredoxin and RhNUDX1 coding sequences. The fusion protein was expressed in *E. coli* BL21-AI strain. After induction with 1 mM IPTG, bacteria were grown overnight at 20°C, lysed by sonication, then the fusion protein was purified by affinity chromatography on Talon® resin (Clontech). Thrombin protease (GE Healthcare life sciences) was incubated overnight at 4°C with the resin-bound fusion protein to recover RhNUDX1. One hundred micrograms of purified RhNUDX1 was subjected to SDS-PAGE for further purification. The band corresponding to RhNUDX1 was cut from the gel, ground in Freund's complete adjuvant (800 µl) and then used for immunization of a New-Zealand rabbit. Western blots were performed according to (40).

#### RhNUDX1 enzyme assay

For enzyme assays and determination of kinetic parameters, purified NusA-RhNUDX1 fusion protein (100-500 ng) was incubated with GPP or FPP, ranging from 0.1 to 50 µM in incubation buffer (50 mM HEPES pH 8, 5 mM MgCl<sub>2</sub>, 1 mM MnCl<sub>2</sub>, 14 mM β-mercaptoethanol, 10% glycerol, v/v) in a final volume of 100 µL for 15 min at 30°C. For each assay, a similar control incubation containing the same amount of heat-inactivated NusA-RhNUDX1 was performed in parallel. The reactions were stopped by addition of 10 µL of EDTA 100 mM pH8 and 90 µL of ethanol containing 0.5% NH<sub>4</sub>OH. RhNUDX1-dependant GP or FP synthesis were calculated after subtracting the GP or FP amounts present in the corresponding control incubation containing the heat-inactivated enzyme. K<sub>m</sub> and K<sub>cat</sub> values were calculated from Lineweaver-Burk plots. For substrate specificity studies, purified NusA-RhNUDX1 (500 ng) was incubated with different substrates (GPP, FPP, dGTP, 8-oxo-dGTP) at a concentration of 20 µM in incubation buffer (100 µL final volume) for 1 h at 30°C. Reaction products were analyzed by LC-MS on an Ultimate 3000 UHPLC system coupled to an Exactive mass spectrometer (Thermo Fischer Scientific, San Jose, USA). Separations were performed on a Nucleodur C18 HTec column (50 x 2 mm i.d., 1.8 µm particle size, Macherey-Nagel, Düren, Germany), operated at 20°C. Mobile phase consisted of 5 mM of ammonium bicarbonate in water (eluent A) and acetonitrile (eluent B). Flow rate was 0.3 mL/min. The elution program was as follows: isocratic for 1.5 min with 1% B, 1-100% B (5 min), isocratic with 100% B (1 min). The sample volume injected was 2 µl. The Exactive Orbitrap mass spectrometer was equipped with an electrospray ionization (ESI) source operating in negative mode. Parameters were set at 300°C for ion transfer capillary temperature and 2500 V for ion spray voltage. Nebulization with nitrogen sheath gas and auxiliary gas were maintained at 50 and 4 arbitrary units, respectively. The spectra were acquired within the *m/z* mass range of 100-800 Da, using a resolution of 50000 at 200 Da. The instrument was operated using the ExactiveTune software and data were processed using the Xcalibur software. The system was calibrated externally using the Thermo Fischer calibration mixture in the range of *m/z* 100-2000 Da, giving a mass accuracy lower than 2 ppm. Reaction products were identified according to their mass spectra and retention time, compared to those of authentic

standards. Quantifications were based on calibration curves obtained with authentic standards.

#### GC and GC-MS analyses of scent compounds and LC-MS analysis of geraniol derivatives

Rose petal scent compounds and monoterpenes produced in tobacco were extracted with hexane and analyzed according to (16). For the analysis of geraniol glycosides in *N. benthamiana*, leaf sectors (1 g) were cut from agroinfiltrated leaves (96 h post infiltration), ground under liquid nitrogen. The resulting powder was then suspended 5 mL of PBS containing 10% ethanol (v/v). Piceid (resveratrol 3- $\beta$ -mono-D-glucoside) was added as an external standard. After a 5-min centrifugation (10000 g at 4°C), the supernatant was collected and applied on a C18 SPE column (Bond Elut Jr., Varian). The column was washed twice with 5 mL of water, and eluted with 2 mL of ethanol/H<sub>2</sub>O (90/10, v/v). This eluted fraction was analyzed by LC-MS using a Nucleodur C18 HTec column (50 x 2 mm) as described above, with the following modifications. Mobile phase consisted of water/formic acid (0.1%, v/v; eluent A) and acetonitrile/formic acid (0.1%, v/v; eluent B). Flow rate was 0.3 mL/min. The elution program was as follows: 20% to 100% B (5 min), isocratic with 100% B (3 min). The sample volume injected was 2  $\mu$ L. The Exactive mass spectrometer operated in positive mode, with parameters set at 300°C for ion transfer capillary temperature and 4500 V for ion spray voltage. Geranyl glycosides were detected using their characteristic fragment ion [C<sub>10</sub>H<sub>17</sub>]<sup>+</sup> (*m/z* 137.1325). The major geranyl glycosides: hexosyl-geraniol (C<sub>16</sub>H<sub>28</sub>O<sub>6</sub>), malonyl-hexosyl-geraniol (C<sub>19</sub>H<sub>30</sub>O<sub>9</sub>) and pentosyl-hexosyl-geraniol (C<sub>21</sub>H<sub>36</sub>O<sub>10</sub>) were quantified as geranyl glucoside equivalent, by integrating the signal corresponding to the [C<sub>10</sub>H<sub>17</sub>]<sup>+</sup> ion. Geranyl  $\beta$ -D-glucoside standard was from Carbosynth (Compton, UK).

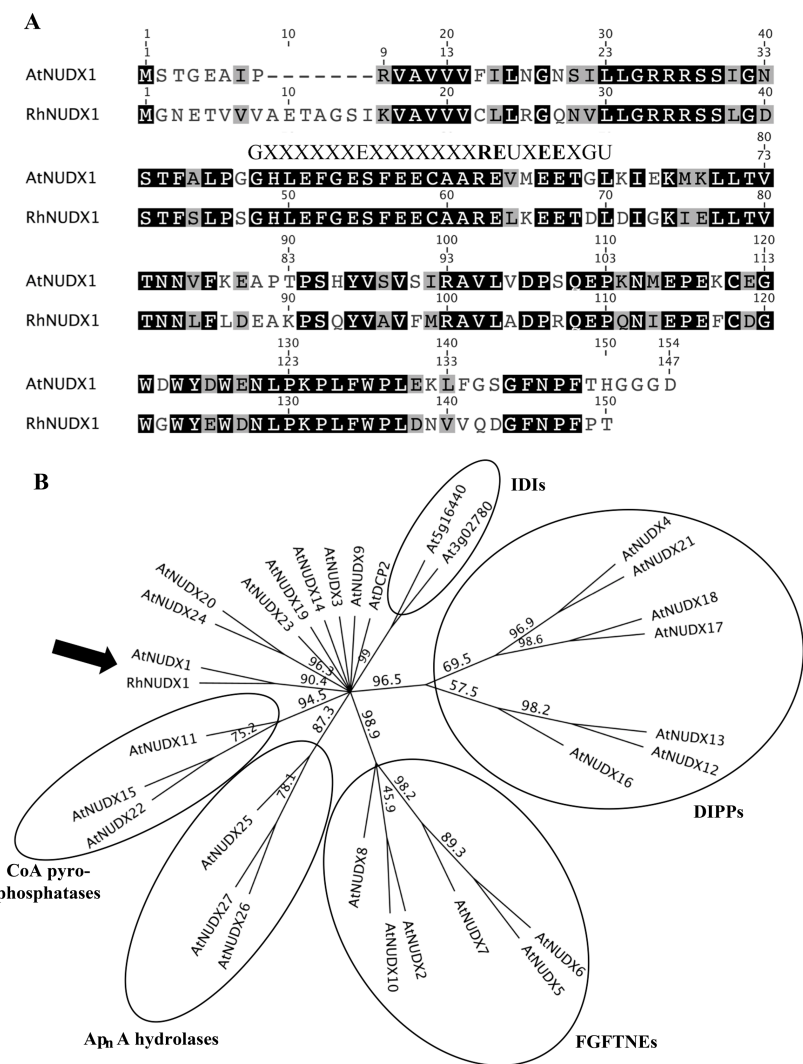


**Fig. S1**

- A.** Alignment of amino acid sequences from *Arabidopsis* (AtNUDX1) and rose (RhNUDX1) performed using ClustalW. Conserved or substitutive amino acids are highlighted in black and gray, respectively. The conserved Nudix box (Gx<sub>5</sub>Ex<sub>7</sub>REUxEExGU with x = any amino acid and U = bulky aliphatic residue (usually I, L or V)) is shown. Similar to AtNUDX1, no signal peptide or transit peptide to either mitochondria or chloroplasts was identified in RhNUDX1 using the TargetP (17) and SignalP (41) prediction software.
- B.** Unrooted Neighbour Joining tree depicting the relationships of RhNUDX1 with the 28 putative *Arabidopsis* Nudix hydrolases. Tree was constructed using Geneious software. Representative bootstrap values are shown as a percentage from 1000 bootstraps replicates. *Arabidopsis* Nudix hydrolases were named according to (42). Nudix subfamilies were defined according to (43). DIPPs, diphosphoinositol polyphosphate phosphohydrolases; FGFTNEs, Fibroblast growth factor type Nudix Enzyme; IDI, Isopentenyl diphosphate Isomerase.

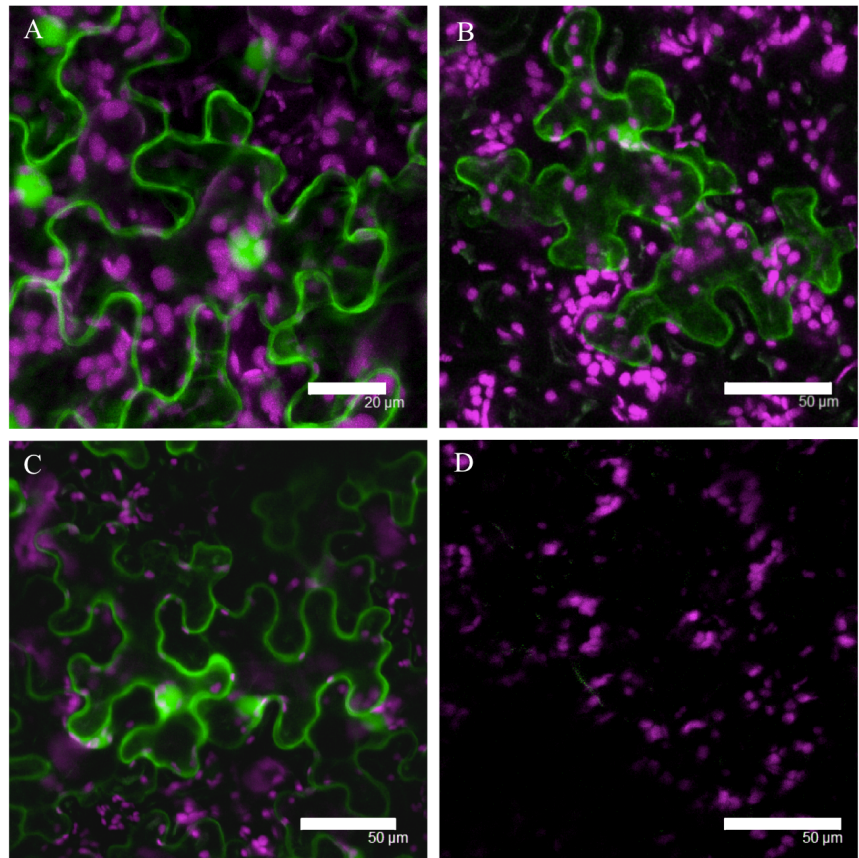


**Fig. S2**

Confocal image projections of transient expression of GFP fusion proteins following transformation of *Nicotiana benthamiana* leaf epidermal cells. **A.** Expression of GFP targeted to cytoplasm; **B.** Expression of RhNUDX1-GFP fusion protein; **C.** Expression of GFP-RhNUDX1 protein; **D.** Cells transformed with p19 construct alone. Bars = 20  $\mu$ m (A) or 50  $\mu$ m (B-D). Green channel, GFP. Purple channel, chlorophyll.

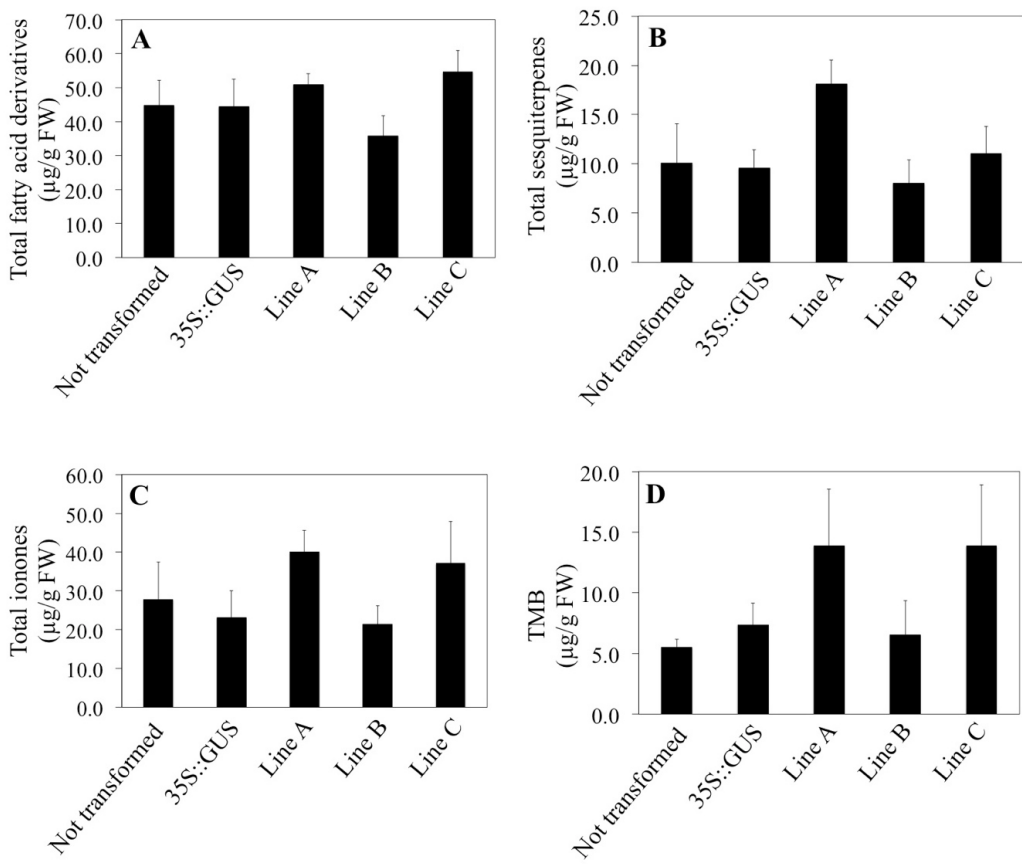


**Fig. S3**

GCMS analyses of the petal volatile compounds in transgenic rose lines. Lines A, B and C, roses transformed with *RNAi-RhNUDX1*. 35S::GUS, roses transformed with the Gus reporter gene under the control of the 35S promoter. **A.** Fatty acid derivatives; **B.** Sesquiterpenes; **C.** Ionones; **D.** 1,3,5-trimethoxybenzene (TMB). Values represent means +/- standard error (n=8 to 12). There was no significant difference between means (Tukey's HDS test, p<0.05).

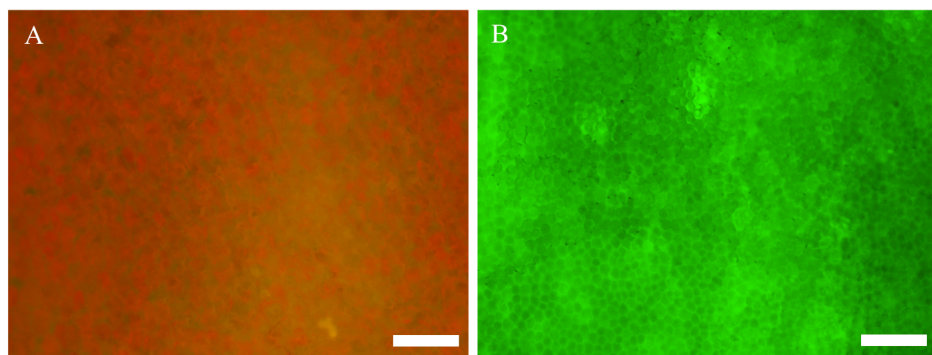


**Fig. S4**

Micrographs of transient expression of GFP fusion proteins following transformation of *Rosa x hybrida* ‘The Mac Cartney rose’ petal cells. **A.** Cells transformed with p19 construct alone. **B.** Co-expression of p19 and GFP targeted to cytoplasm; Bars = 150  $\mu\text{m}$ .

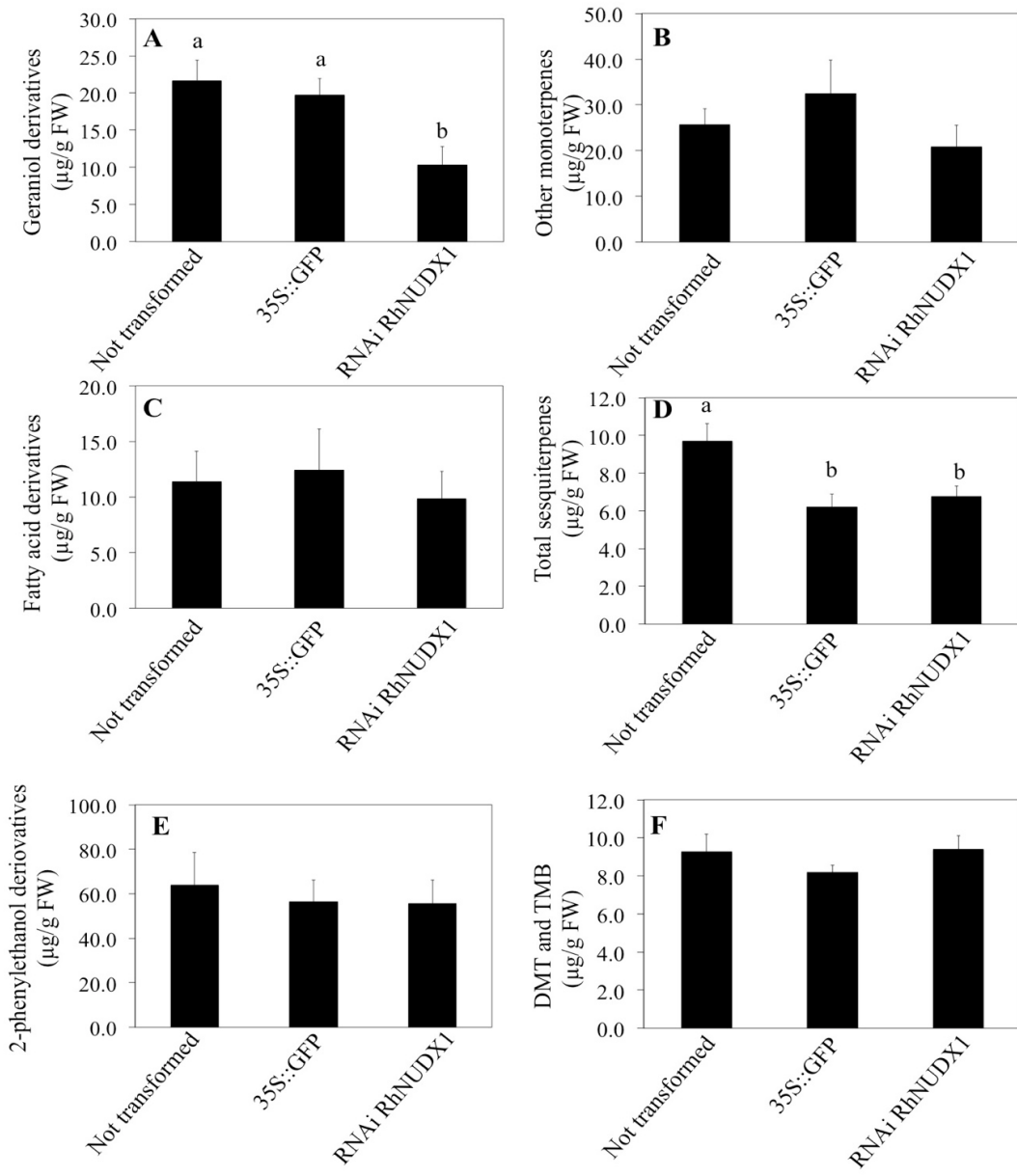


**Fig. S5**

GC-MS analysis of the volatile compounds in transiently transformed rose petals of the ‘The Mac Cartney rose’ cultivar. Volatiles are expressed in  $\mu\text{g}$  per g of fresh weight (averages of 6 different replicates). *RNAi RhNUDX1*, petals transformed with *RNAi-RhNUDX1*. *35S::GFP* construct, petals transformed with a construct harboring the Green Fluorescent protein gene under the control of the 35S promoter. **A.** Geraniol derivatives; **B.** Other monoterpenes; **C.** Fatty acid derivatives; **D.** sesquiterpenes; **E.** 2-phenylethanol derivatives; **F.** DMT and 1,3,5-trimethoxybenzene (TMB). Means with different letters are significantly different (Tukey’s HDS test,  $p<0.05$ ).

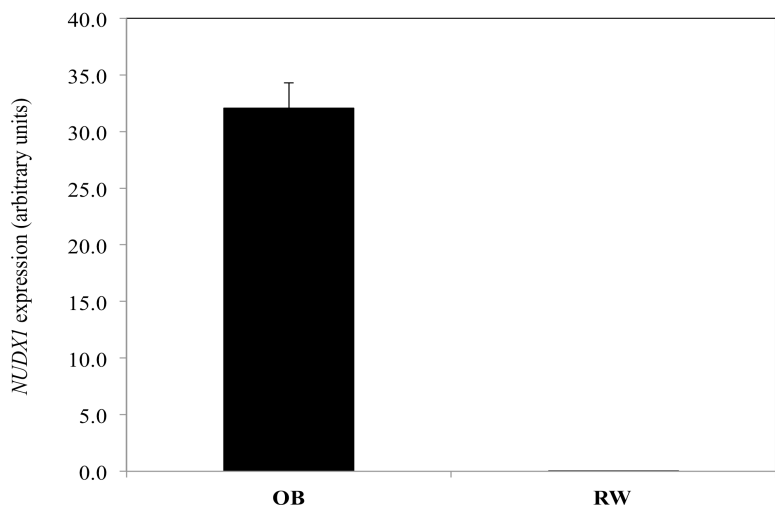


**Fig. S6**

Expression level of *NUDX1* in petals of *R. wichurana* (RW) and *R. chinensis* cv. ‘Old Blush’ (OB). Transcript levels of *NUDX1* were normalized to genes coding for  $\alpha$ -tubulin and EF1- $\alpha$  according to (27). Error bars indicate SE obtained from two independent biological replicates. Two technical replicates were performed for each biological replicate.

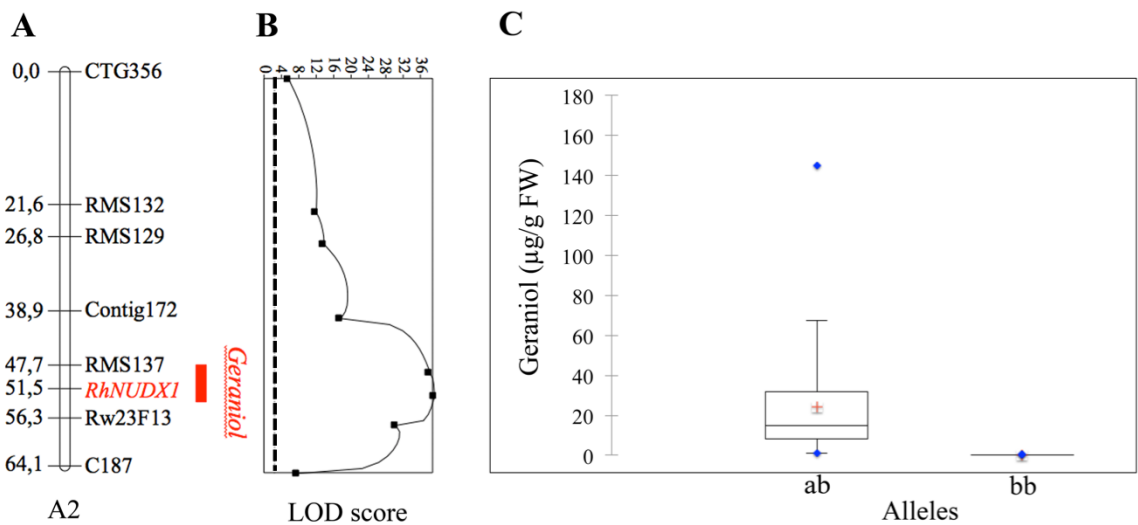


**Fig. S7**

A QTL for geraniol production colocalized with *NUDX1* on the female linkage group 2 (A2) of the OW progeny. **A.** Genetic map based on SSR and *RhNUDX1* CAPS markers. The distances are indicated in cM. **B.** LOD score curve from interval mapping analysis. Dashed line shows genome-wide significant threshold based on permutation test. The one-LOD confidence interval is indicated with a red filled bar. **C.** Boxplots of geraniol contents in petals of the OW progeny, as a function of the genotype at the *NUDX1* locus (alleles ab or bb). Red crosses represent the means, lines within the box represent the medians and blue rhombuses correspond to the minimum and maximum values.

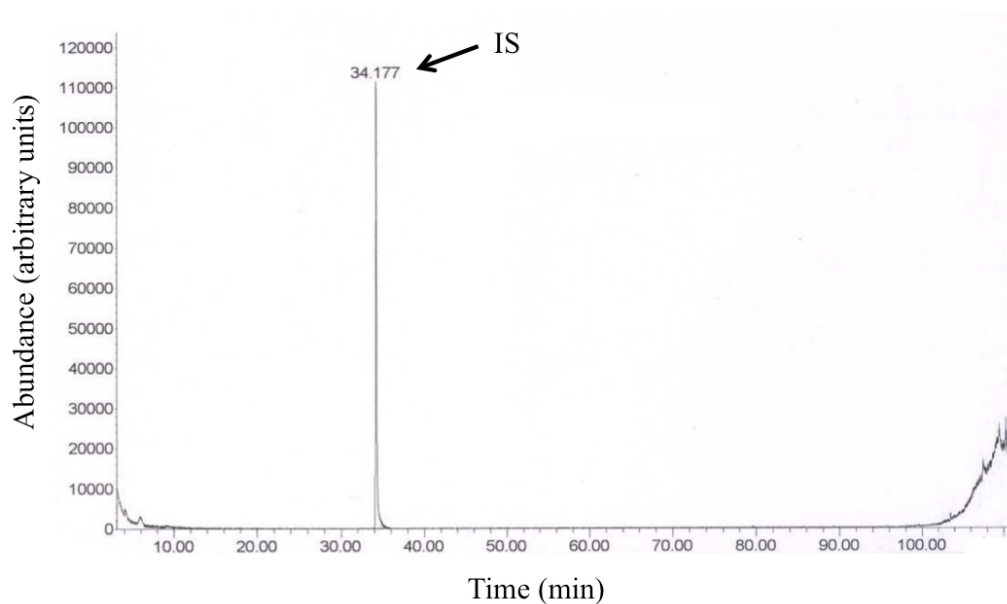


**Fig. S8**

GC-MS analysis of recombinant RhNUDX1 activity.

4  $\mu$ g of native NusA-RhNUDX1 fusion protein were assayed in the presence of 100  $\mu$ M GPP, HEPES 50mM pH 8, 5 mM MgCl<sub>2</sub>, 1 mM MnCl<sub>2</sub>, 1 mM DTT in a final volume of 100  $\mu$ L for 4 h at 30°C. IS, internal standard (camphor).

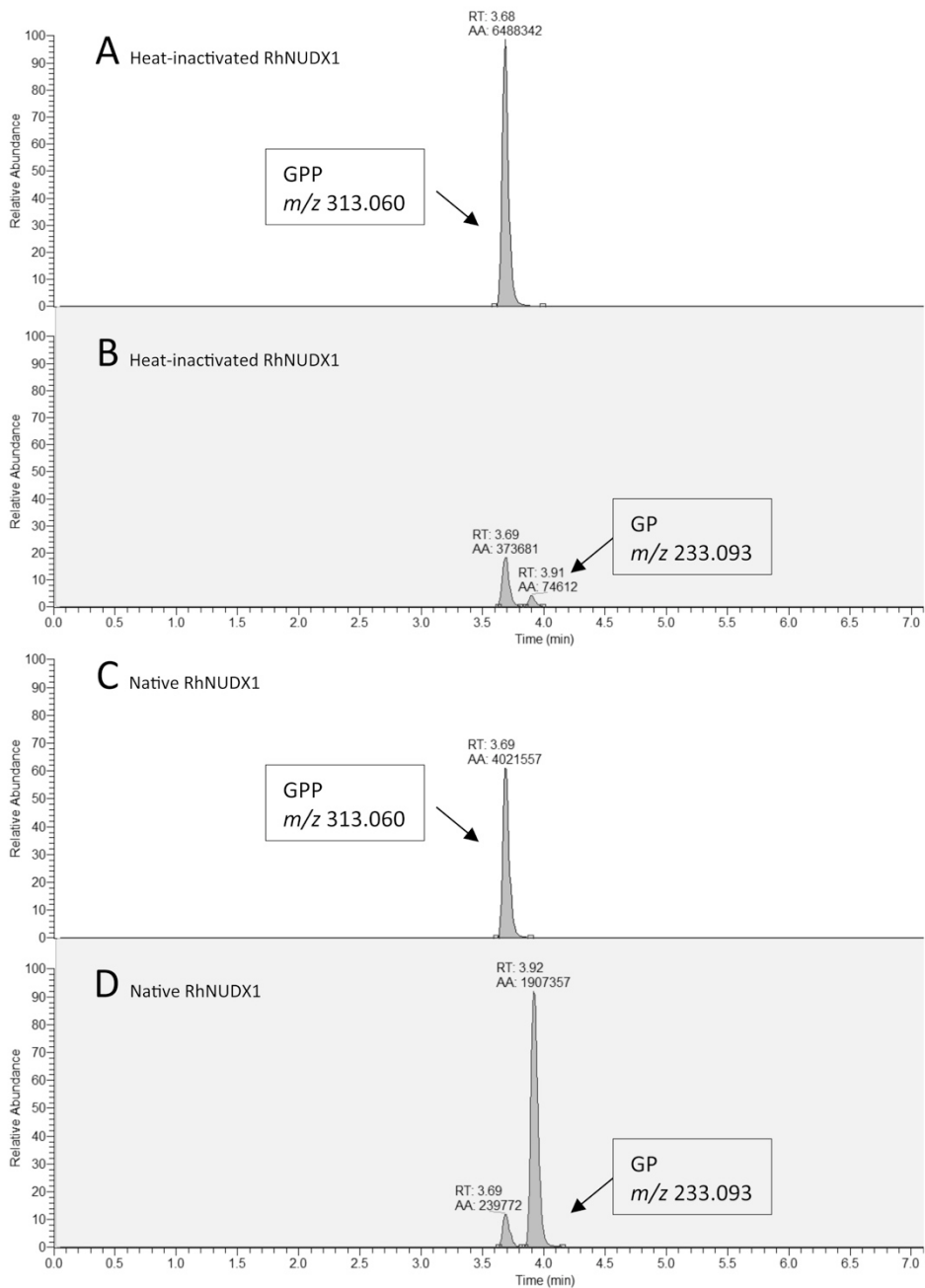


**Fig. S9**

LC-MS analysis of recombinant RhNUDX1 activity.

500 ng of heat inactivated (A, B) or native NusA-RhNUDX1 fusion protein (C, D) were assayed in the presence of 3  $\mu$ M GPP, 5 mM MgCl<sub>2</sub>, 1 mM MnCl<sub>2</sub>, 14 mM  $\beta$ -mercaptoethanol, 10% glycerol (v/v) in a final volume of 100  $\mu$ L for 30 min at 30°C. Reaction products were analyzed by LC-MS. Panels A and C present the extracted ion chromatograms for  $m/z$  313.060 ( $[GPP-H]^-$  ion) corresponding to GPP. Panels B and D present the extracted ion chromatograms for  $m/z$  233.093 ( $[GP-H]^-$  ion) corresponding to GP. Relative abundance scales are identical in A and C, and in B and D, respectively. Retention times (RT) and peak areas (AA) are indicated.

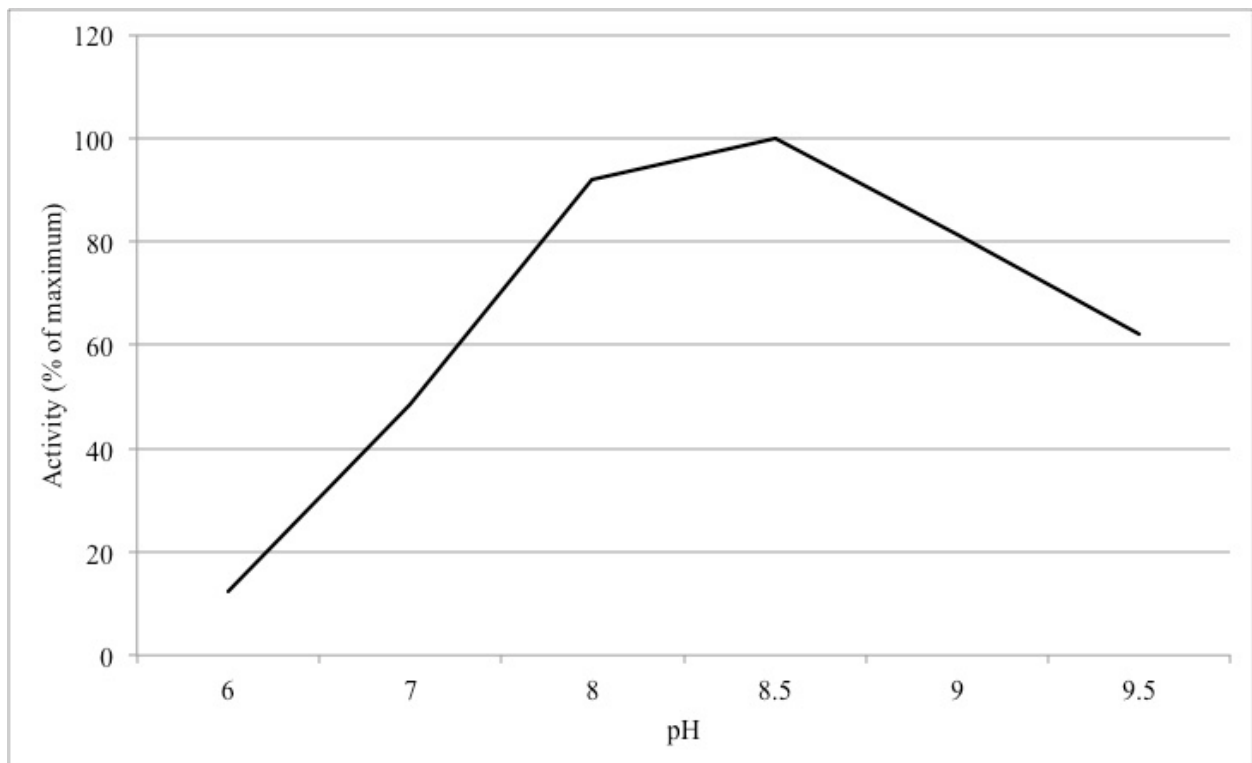


**Fig. S10**

pH dependency of RhNUDX1 activity *in vitro*. NusA-RhNUDX1 was assayed in the presence of 3 µM GPP, 5 mM MgCl<sub>2</sub>, 1 mM MnCl<sub>2</sub>, 14 mM β-mercaptoethanol, 10% glycerol (v/v) in a final volume of 100 µL for 15 min at 30°C. Assays contained either 50 mM Mes (pH 6.0), 50 mM Hepes (pH 7.0 and pH 8.0), 50 mM Tris (pH 8.5) or 50 mM Capso (pH 9 and 9.5) as buffer.

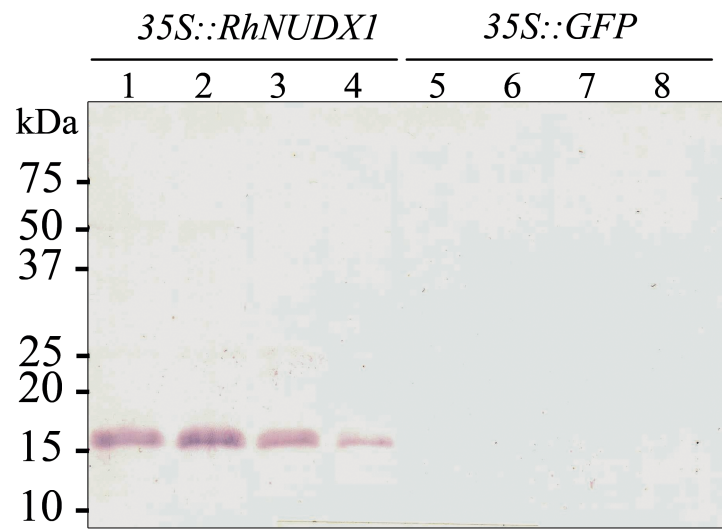


**Fig. S11**

Western blot analysis of RhNUDX1 protein in *Nicotiana benthamiana* leaves. 1 to 4, leaves infiltrated with Agrobacteria carrying 35S::RhNUDX1; 5 to 8, leaves transiently transformed with Agrobacteria carrying the 35S::GFP construct.

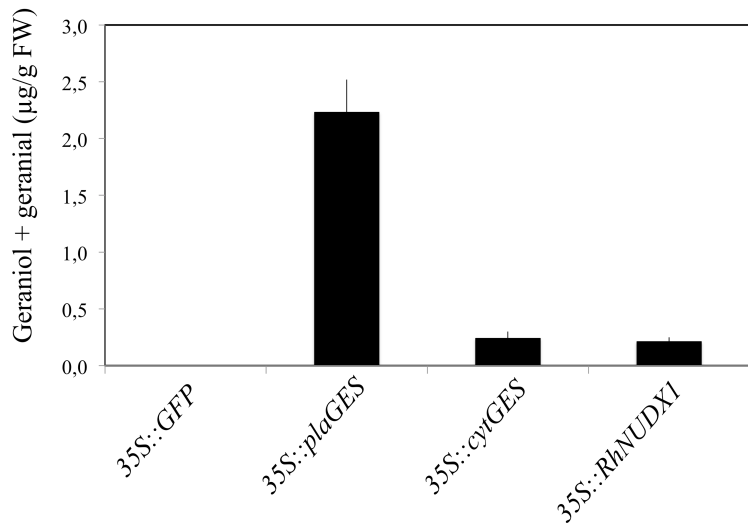


**Fig. S12**

Geraniol and geranial accumulation following transient expression of *RhNUDX1* in *N. benthamiana*. GES from basil (9) was expressed as a full-length protein including its transit peptide (Plastidic GES, 35S::plaGES) and as a truncated protein without transit peptide (Cytosolic GES, 35S::cytGES). GFP was used as a control. 96 h after transformation, geraniol and geranial were quantified by GC-MS. Data are expressed in  $\mu\text{g}$  per g fresh leaf weight (gFW), as means of triplicate assays and bars indicate SE.

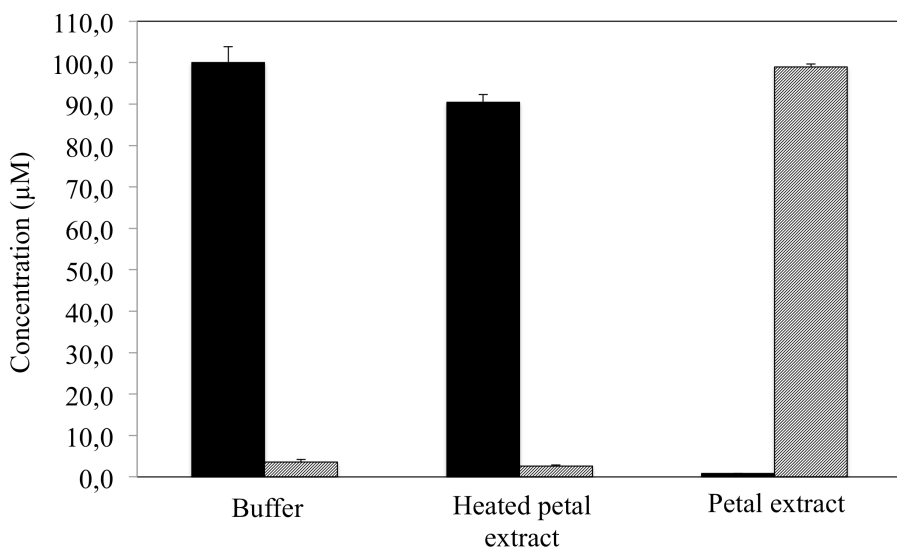


**Fig. S13**

Geranyl monophosphate (GP) phosphohydrolase activity in rose petals.

5 g of petals from *Rosa x hybrida* cv. White Naomi were homogenized in 15 mL citrate buffer 100 mM pH5 containing 1% of PVPP and centrifuged for 15 min at 15000 g to yield the rose petal crude extract. Petal crude extract (100 μL), heated petal extract (100°C, 10 min) or citrate buffer (100 μL) were incubated in the presence of GP (100 μM) for 8 h. The resulting incubation mixtures were analyzed using LC-MS in positive-negative switching mode, for the presence of GP ( $[GP-H]^-$  ion,  $m/z$  233.093, retention time 3.79 min) and geraniol ( $[C_{10}H_{17}]^+$  ion,  $m/z$  137.1325, retention time 5.88 min). Histograms show GP and geraniol concentrations in black and in grey, respectively. Analyses were performed on 3 independent incubations of each kind and bars indicate SE.

**Table S1.**

Major volatile compounds extracted from petals of 10 rose cultivars at fully opened flower stage and analyzed by GC-FID. <sup>a</sup>Values represent relative proportion of total peak area (averages of 3 to 7 different replicates). Only compounds present in the headspace were taken into account. Total volatiles are expressed in µg per g of fresh weight +/- SE. PM, ‘Papa Meilland’; RM, ‘Rouge Meilland’; AL, ‘Alister Stella Grey’; HA, ‘Hacienda’; PC, ‘Pariser Charme’; OB, ‘Old Blush’; AN, ‘Anna’; MU, ‘Mutabilis’; BB, ‘Black Baccara’; BA, ‘Baccara’. BAL, benzyl alcohol and benzaldehyde; CIT, citronellol; DMT, 3,5-dimethoxytoluene; EUG, eugenol and methyleugenol; FAD, hexanal, E-2-hexenal, Z-3-hexenol, E-2-hexenol, 1-hexanol, Z-3-hexenyl acetate, hexyl acetate and nonanal; FAR, E-β-farnesene, farnesol, farnesal and farnesyl acetate; GEM, germacrene D, germacrene D-4-ol and bicyclogermacrene; GER, geraniol, geranial, geranic acid and geranyl acetate; ION, 3,4-dihydro-β-ionone and dihydro-β-ionol; MON, β-myrcene, Z-β-ocimene and E-β-ocimene; NER, nerol and neral; PHE, 2-phenylethanol and phenylacetaldehyde; SES, δ-cadinene, elemol, α-cadinol, τ-cadinol and τ-muurolol; TMB, 1,3,5-trimethoxybenzene.

Compounds	Rose cultivars									
	PM	RM	AL	HA	PC	OB	AN	MU	BA	BB
FAD	1.6 <sup>a</sup>	53.1	0.2	2.0	2.3	24.1	9.2	7.5	33.7	34.2
hexanal	0.6	7.3	0.1	0.7	0.5	0.5	1.5	0.7	2.0	9.7
E-2-hexenal	0.8	22.4	0.1	1.0	1.0	9.6	6.5	3.6	4.1	8.0
Z-3-hexenol	0.0	6.8	0.0	0.0	0.0	4.6	0.0	0.0	10.1	8.1
E-2-hexenol	0.0	1.5	0.0	0.0	0.0	1.8	0.0	0.0	1.8	0.8
1-hexanol	0.1	6.9	0.0	0.1	0.0	0.4	0.0	0.0	4.0	2.5
Z-3-hexenyl acetate	0.1	5.7	0.0	0.1	0.4	7.1	0.7	2.8	9.3	2.6
hexyl acetate	0.0	0.6	0.0	0.1	0.1	0.0	0.4	0.1	0.8	0.0
nonanal	0.0	1.9	0.0	0.0	0.3	0.1	0.1	0.3	1.6	2.5
BAL	1.2	14.1	0.6	1.0	2.5	0.1	0.6	0.3	24.6	46.8
benzyl alcohol	1.1	13.9	0.3	0.9	2.3	0.1	0.6	0.3	24.1	34.5
benzaldehyde	0.1	0.2	0.3	0.1	0.2	0.0	0.0	0.0	0.5	12.3
PHE	12.7	0.0	80.5	47.1	0.1	0.4	0.0	0.6	3.5	4.5
2-phenylethanol	12.0	0.0	68.9	44.3	0.1	0.4	0.0	0.5	3.4	3.9
phenylacetaldehyde	0.7	0.0	11.6	2.8	0.0	0.0	0.0	0.1	0.1	0.5
DMT	0.6	24.3	0.1	1.6	0.0	0.1	15.8	0.6	7.1	11.7
TMB	0.2	0.6	0.0	0.0	0.0	9.7	0.0	1.1	4.3	0.0

EUG	0.1	1.0	1.2	0.3	5.8	0.0	0.6	0.0	0.1	0.0
eugenol	0.0	1.0	1.1	0.2	5.5	0.0	0.2	0.0	0.1	0.0
methyleugenol	0.1	0.0	0.1	0.1	0.3	0.0	0.4	0.0	0.0	0.0
GER	63.4	2.0	14.2	28.7	48.1	44.4	0.1	74.4	3.4	2.8
geraniol	49.5	1.9	9.8	20.6	29.7	38.1	0.1	60.2	3.0	2.1
geranial	9.9	0.1	2.6	6.3	13.8	6.1	0.0	13.4	0.4	0.7
geranic acid	3.6	0.0	1.4	1.2	3.7	0.0	0.0	0.0	0.0	0.0
geranyl acetate	0.4	0.0	0.4	0.6	0.9	0.2	0.0	0.8	0.0	0.0
NER	6.6	0.0	1.2	3.3	15.5	0.2	0.0	3.3	0.2	0.0
nerol	6.1	0.0	1.0	2.7	13.7	0.1	0.0	2.6	0.2	0.0
neral	0.5	0.0	0.2	0.6	1.8	0.1	0.0	0.7	0.0	0.0
CIT	3.7	0.0	0.6	6.9	5.5	0.6	0.0	0.0	0.6	0.0
MON	0.2	0.0	0.0	1.0	3.8	0.0	0.1	0.1	0.0	0.0
$\beta$ -myrcene	0.1	0.0	0.0	0.6	2.3	0.0	0.0	0.1	0.0	0.0
Z- $\beta$ -ocimene	0.0	0.0	0.0	0.1	0.5	0.0	0.0	0.0	0.0	0.0
E- $\beta$ -ocimene	0.1	0.0	0.0	0.3	1.0	0.0	0.1	0.0	0.0	0.0
GEM	0.4	0.0	0.6	1.2	3.3	8.1	45.3	7.7	12.6	0.0
germacrene D	0.4	0.0	0.4	1.1	2.9	7.5	44.5	6.9	12.3	0.0
germacrene D-4-ol	0.0	0.0	0.2	0.0	0.3	0.6	0.2	0.7	0.0	0.0
bicyclogermacrene	0.0	0.0	0.0	0.1	0.1	0.0	0.7	0.1	0.3	0.0
FAR	9.2	4.1	0.5	6.1	5.9	0.1	0.0	0.8	0.5	0.0
E- $\beta$ -farnesene	0.3	0.6	0.0	0.5	1.1	0.0	0.0	0.0	0.2	0.0
farnesol	8.6	3.5	0.4	5.1	4.7	0.1	0.0	0.8	0.3	0.0
farnesal	0.2	0.0	0.0	0.1	0.1	0.0	0.0	0.0	0.0	0.0
farnesyl acetate	0.1	0.0	0.1	0.4	0.0	0.0	0.0	0.0	0.0	0.0
SES	0.1	0.0	0.1	0.8	3.8	0.6	8.5	0.7	3.2	0.0
$\delta$ -cadinene	0.0	0.0	0.0	0.3	0.4	0.2	2.1	0.4	1.4	0.0
$\alpha$ -cadinol	0.1	0.0	0.0	0.3	0.9	0.2	3.2	0.2	1.0	0.0
$\tau$ -cadinol	0.0	0.0	0.0	0.1	0.3	0.0	1.2	0.0	0.5	0.0

$\tau$ -muurolol	0.0	0.0	0.1	0.1	0.8	0.2	2.0	0.1	0.3	0.0
elemol	0.0	0.0	0.0	0.0	1.3	0.0	0.0	0.0	0.0	0.0
ION	0.1	0.8	0.4	0.0	3.3	11.7	19.8	2.9	6.2	0.0
3,4-dihydro- $\beta$ -ionone	0.0	0.6	0.1	0.0	0.1	0.1	5.5	0.1	0.1	0.0
dihydro- $\beta$ -ionol	0.1	0.2	0.3	0.0	3.2	11.6	14.3	2.8	6.1	0.0
Total volatiles	324.4 +/- 36.8	27.0 +/- 2.7	885.8 +/- 170.7	345.8 +/- 42.6	170.3 +/- 24.9	167.2 +/- 26.6	162.2 +/- 38.7	144.7 +/- 17.1	45.7 +/- 3.8	22.8 +/- 1.8

**Table S2.**

List of 21 genes whose expression is upregulated in ‘Papa Meilland’, PM compared to ‘Rouge Meilland’, RM as revealed by microarray and cDNA AFLP analyses and expression of candidate genes in petals of 10 different rose cultivars at fully opened flower stage, analyzed by qPCR. <sup>a</sup>For microarray, fold increase represent the ratio of the mean sum intensity of two biological replicates for one probe set. NC, not calculated. <sup>b</sup>For qPCR analyses, values represent the relative quantity of cDNA, with expression in RM stated as 1. Expression was normalized with *RhTUB* and *RhEF1a* genes. AL, ‘Alister Stella Grey’; HA, ‘Hacienda’; PC, ‘Pariser Charme’; OB, ‘Old Blush’; AN, ‘Anna’; MU, ‘Mutabilis’; BB, ‘Black Baccara’; BA, ‘Baccara’.

Clone n°	Accession number	Blast result	Microarray fold increase PM/RM <sup>a</sup>	Relative expression of the candidate genes in the rose cultivars analyzed by qPCR <sup>b</sup>									
				PM	RM	AL	HA	PC	OB	AN	MU	BA	BB
<i>RhNUDX1/PM1</i>	JQ820249	Nudix hydrolase	7583	6980.1	1.0	4734.0	17962.0	7379.0	2334.6	0.1	5663.9	0.5	87.0
<b>DIF1</b>													
PM3	EC586313	No significant homology	375	3.1	1.0	0.1	8.9	1.2	0.8	0.0	0.1	12.5	14.4
PM4	EC586128	Peptidyl-prolyl isomerase	330	1133.0	1.0	182.9	1141.9	71.5	538.8	595.8	879.0	239.2	88.3
PM5	BQ105401	UDP-glucosyltransferase	262	108.8	1.0	7.9	2.3	5.5	1.6	2.1	6.6	3.7	157.7
PM6	BI977820	Aldoketoreductase	249	1308.8	1.0	146.0	91.8	2904.1	1.7	7.7	61.7	316.2	370.5
PM9	BI978145	Metal ion binding protein	109	5.1	1.0	13.5	6.6	29.8	7.3	5.0	12.6	10.6	11.8
PM10	BQ106431	Long chain fatty alcohol oxidase	63	28.7	1.0	0.3	0.5	51.6	0.8	1.1	1.7	0.4	2.7
PM13	BQ104744	BRH1 RING finger protein	24	7.2	1.0	13.9	9.0	9.7	2.1	3.2	18.8	2.3	0.9
PM19	BI978913	No significant homology	20	3.8	1.0	24.4	3.8	9.9	71.7	0.9	78.6	2.8	0.7
PM20	BQ104568	PREG1-like negative regulator	27	2.9	1.0	5.8	43	1.2	8.6	6.1	22.6	0.0	0.0
PM29	BQ106437	Hypothetical protein <i>A. thaliana</i>	16	7.2	1.0	10.1	3.1	4.0	3.2	3.3	12.8	1.1	1.5
PM35	BQ106017	R-oxynitrile lyase	11	7.1	1.0	1.4	0.5	0.0	0.3	0.3	1.3	0.0	0.1

		isoenzyme 1											
PM36	EC586532	Delta24-sterol-C-methyltransferase	10	6.9	1.0	2.4	2.6	7.1	1.8	2.0	9.0	0.1	0.3
PM45	BQ105260	Heat shock protein	11	4.9	1.0	0.7	2.8	0.5	0.5	1.3	2.6	0.4	0.6
PM46	BQ104892	Common plant regulatory factor	7	4.8	1.0	42.2	3.7	7.2	6.9	5.7	15.4	3.0	4.2
PM47	EC587456	Triterpene UDP-Glucosyl transferase	7	2.8	1.0	1.2	1.6	1.6	1.6	4.3	3.3	0.7	3.0
PM51	BQ104199	MYBR2 transcription factor	11	1.1	1.0	29.7	7.1	3.9	11.1	7.3	21.1	9.1	11.5
PM67	BQ105660	Cytochrome P450-like protein	8	5.1	1.0	0.8	0.6	0.2	0.1	0.7	0.3	0.4	1.3
PM84	BI977979	Auxin-responsive protein	5	1.4	1.0	4.0	5.3	1.1	7.4	2.7	35.4	0.4	2.4
PM88	BQ105775	Short-chain alcohol dehydrogenase like protein	5	3.7	1.0	0.4	4.3	2.4	0.7	1.5	1.4	0.4	0.1
DIF38	EU603403	Putative laccase	NC	48.4	1.0	93.9	26.1	53.5	0.2	39.6	267.8	384.6	240.9

**Table S3.**

Major volatile terpenes extracted from petals of *RNAi-RhNUDX1* transgenic rose lines A, B and C and analyzed by GC-FID and GCMS. <sup>a</sup>Volatile compounds are expressed in µg per g of fresh weight +/- SE (averages of 8 to 12 different replicates). <sup>b</sup>geraniol derivatives : geraniol, geranal, geranyl acetate, nerol, neral, citronellol and citronellal. NT, not transformed.

Compounds	NT	35S::GUS	Line A	Line B	Line C
Total monoterpenes	17.5 <sup>a</sup> +/- 4.6	25.3 +/- 4.9	0.6 +/- 0.1	20.2 +/- 8.5	28.1 +/- 6.6
Total geraniol derivatives <sup>b</sup>	16.4 +/- 4.6	25.0 +/- 4.9	0.6 +/- 0.1	19.6 +/- 8.6	26.8 +/- 6.6
geraniol	12.4 +/- 4.1	20.4 +/- 3.9	0.4 +/- 0.1	15.3 +/- 7.2	20.1 +/- 5.4
geranal	1.5 +/- 0.7	4.1 +/- 0.9	0.2 +/- 0.0	2.5 +/- 1.4	2.6 +/- 1.3
geranyl acetate	1.4 +/- 0.4	0.2 +/- 0.1	0.0 +/- 0.0	0.9 +/- 0.4	2.2 +/- 0.5
nerol	0.3 +/- 0.1	0.1 +/- 0.0	0.0 +/- 0.0	0.2 +/- 0.1	0.5 +/- 0.2
neral	0.0 +/- 0.0	0.1 +/- 0.1	0.0 +/- 0.0	0.1 +/- 0.1	0.1 +/- 0.1
citronellol	0.5 +/- 0.2	0.2 +/- 0.1	0.0 +/- 0.0	0.4 +/- 0.1	0.7 +/- 0.2
citronellal	0.3 +/- 0.1	0.0 +/- 0.0	0.0 +/- 0.0	0.2 +/- 0.1	0.6 +/- 0.2
linalool	0.1 +/- 0.0	0.0 +/- 0.0	0.0 +/- 0.0	0.1 +/- 0.0	0.2 +/- 0.1
limonene	0.7 +/- 0.3	0.0 +/- 0.0	0.0 +/- 0.0	0.3 +/- 0.2	0.9 +/- 0.3
β-myrcene	0.1 +/- 0.0	0.2 +/- 0.1	0.0 +/- 0.0	0.0 +/- 0.0	0.1 +/- 0.0
β-pinene	0.1 +/- 0.1	0.0 +/- 0.0	0.0 +/- 0.0	0.2 +/- 0.1	0.2 +/- 0.0
α-pinene	0.1 +/- 0.0	0.0 +/- 0.0	0.0 +/- 0.0	0.0 +/- 0.0	0.1 +/- 0.1
Total sesquiterpenes	10.1 +/- 4.0	9.5 +/- 1.9	18.3 +/- 2.5	8.3 +/- 2.4	11.5 +/- 2.7
β-elemene	0.1 +/- 0.0	0.1 +/- 0.1	0.1 +/- 0.0	0.1 +/- 0.0	0.2 +/- 0.1
β-caryophyllene	0.0 +/- 0.0	0.0 +/- 0.0	0.2 +/- 0.0	0.0 +/- 0.0	0.2 +/- 0.1
α-humulene	0.3 +/- 0.2	0.0 +/- 0.0	0.3 +/- 0.1	0.0 +/- 0.0	0.1 +/- 0.0
α-muurolene	0.4 +/- 0.2	0.0 +/- 0.0	0.3 +/- 0.1	0.1 +/- 0.0	0.3 +/- 0.1
germacrene D	5.2 +/- 2.5	4.5 +/- 1.0	9.2 +/- 1.7	3.5 +/- 1.0	4.9 +/- 1.3
bicyclogermacrene	0.2 +/- 0.2	0.0 +/- 0.0	0.4 +/- 0.2	0.0 +/- 0.0	0.2 +/- 0.1
E,E α-farnesene	0.2 +/- 0.1	0.0 +/- 0.0	0.4 +/- 0.1	0.1 +/- 0.1	0.3 +/- 0.1
Δ-cadinene	0.6 +/- 0.3	0.2 +/- 0.1	0.9 +/- 0.2	0.3 +/- 0.1	0.7 +/- 0.1
unknown	0.2 +/- 0.1	0.0 +/- 0.0	0.2 +/- 0.1	0.1 +/- 0.0	0.1 +/- 0.1
sesquiterpene					
germacrene D-4-ol	0.7 +/- 0.2	2.1 +/- 0.4	1.8 +/- 0.1	1.4 +/- 0.5	1.0 +/- 0.4
T-cadinol	0.6 +/- 0.2	0.1 +/- 0.1	1.0 +/- 0.1	0.4 +/- 0.1	0.8 +/- 0.2
T-muurolol	0.3 +/- 0.1	1.0 +/- 0.2	1.0 +/- 0.0	0.9 +/- 0.4	0.5 +/- 0.3
α-muurolol	0.0 +/- 0.0	0.1 +/- 0.0	0.3 +/- 0.0	0.2 +/- 0.1	0.4 +/- 0.1
α-cadinol	1.2 +/- 0.3	1.1 +/- 0.2	2.1 +/- 0.1	0.9 +/- 0.2	1.7 +/- 0.4
Farnesol	0.0 +/- 0.0	0.3 +/- 0.2	0.1 +/- 0.0	0.1 +/- 0.1	0.1 +/- 0.1

**Table S4.**

Major volatile terpenes extracted from transiently transformed petals of ‘The Mac Cartney rose’ cultivar and analyzed by GC-FID and GCMS. <sup>a</sup>Volatile compounds are expressed in µg per g of fresh weight +/- SE (averages of 6 different replicates). <sup>b</sup>geraniol derivatives : geraniol, geranial, geranyl acetate, nerol, neral, citronellol and citronellal. NT, not transformed.

Compounds	NT	<i>35S::GFP</i>	<i>RNAi-RhNUDX1</i>
Total monoterpenes	47.4 <sup>a</sup> +/- 3.1	52.2 +/- 7.0	31.1 +/- 6.8
Total geraniol derivatives <sup>b</sup>	21.7 +/- 2.7	19.7 +/- 2.3	10.3 +/- 2.5
geraniol	0.4 +/- 0.2	0.3 +/- 0.1	0.1 +/- 0.1
nerol	7.5 +/- 0.6	7.0 +/- 0.9	3.5 +/- 1.0
neral	0.4 +/- 0.2	0.6 +/- 0.2	0.3 +/- 0.1
neryl acetate	1.6 +/- 0.9	0.0 +/- 0.0	0.0 +/- 0.0
citronellol	11.6 +/- 1.5	11.8 +/- 1.1	6.4 +/- 1.4
citronellyl acetate	0.1 +/- 0.1	0.1 +/- 0.1	0.0 +/- 0.0
limonene	4.0 +/- 0.4	5.2 +/- 1.0	3.8 +/- 0.4
β-myrcene	12.2 +/- 1.5	14.3 +/- 2.9	10.2 +/- 2.0
α-phellandrene	0.0 +/- 0.0	0.2 +/- 0.2	0.0 +/- 0.0
α-terpinene	0.2 +/- 0.1	0.6 +/- 0.2	0.2 +/- 0.1
γ-terpinene	0.0 +/- 0.0	0.4 +/- 0.2	0.1 +/- 0.1
α-terpinolene	1.1 +/- 0.1	1.4 +/- 0.2	1.0 +/- 0.1
Z-β-Ocimene	3.2 +/- 0.3	3.9 +/- 0.7	2.5 +/- 0.5
E-β-Ocimene	4.1 +/- 1.3	5.6 +/- 2.0	2.4 +/- 1.5
allo-ocimene	0.8 +/- 0.1	1.0 +/- 0.3	0.6 +/- 0.2
Total sesquiterpenes	9.7 +/- 1.0	6.2 +/- 0.7	6.8 +/- 0.5
germacrene D	6.5 +/- 0.8	4.1 +/- 0.3	5.0 +/- 0.4
E-β-farnesene	0.1 +/- 0.1	0.1 +/- 0.1	0.1 +/- 0.1
Δ-cadinene	2.3 +/- 0.2	1.6 +/- 0.1	1.7 +/- 0.2
T-cadinol	0.7 +/- 0.2	0.5 +/- 0.3	0.0 +/- 0.0

**Table S5.**

Kinetic parameters of RhNUDX1 with potential substrates. Data are expressed as the means of triplicates assays using NusA-RhNUDX1 and standard errors are indicated between brackets; n.d.: not determined, as too little activity was observed with these substrates.

	Km (nM)	Kcat (s <sup>-1</sup> )	Kcat/Km (M <sup>-1</sup> .s <sup>-1</sup> )
GPP	140 (30)	0.02 (0.001)	143000
FPP	480 (80)	0.0033 (0.0005)	6875
dGTP	n.d.	n.d.	n.d.
8-oxo-dGTP	n.d.	n.d.	n.d.

## Additional Data (separate files)

### Dataset S1

List of ESTs whose expression is up regulated in ‘Papa Meilland’ versus ‘Rouge Meilland’ (PM1/*RhNUDX1* to PM91) or up regulated in ‘Rouge Meilland’ versus ‘Papa Meilland’ (RM1 to RM134) as revealed by microarray analyses of 5175 unique sequences (2 biological replicates). Values represent Log2 ratios. A gene is declared differentially expressed if the Bonferroni P-Value is less than 0.05. Gene Ontologies annotations (GOs) were assigned to the genes that were up regulated in ‘Papa Meilland’ with Blast 2 go software (44).

### Dataset S2

Correlation matrix of the expression of 21 genes, analyzed by qPCR on petals, and floral scent composition of 10 rose cultivars (AN, ‘Anna’; OB, ‘Old Blush’; PM, ‘Papa Meilland’; RM, ‘Rouge Meilland’; BA, ‘Baccara’; BB, ‘Black Baccara’; AL, ‘Alister Stella Grey’; MU, ‘Mutabilis’; PC, ‘Pariser Charme’; HA, ‘Hacienda’). For each cultivar, 3 to 7 replicates were sampled. A non-parametric Spearman correlation was used.

Correlation coefficients are indicated. Values in bold are significant ( $p < 0.05$ ). BAL, benzyl alcohol and benzaldehyde; CIT, citronellol; DMT, 3,5-dimethoxytoluene; EUG, eugenol and methyleugenol; FAD, hexanal, E-2-hexenal, Z-3-hexenol, E-2-hexenol, 1-hexanol, Z-3-hexenyl acetate, hexyl acetate and nonanal; FAR, E- $\beta$ -farnesene, farnesol, farnesal and farnesyl acetate; GEM, germacrene D, germacrene D-4-ol and bicyclogermacrene; GER, geraniol, geranial, geranic acid and geranyl acetate; ION, 3,4-dihydro- $\beta$ -ionone and dihydro- $\beta$ -ionol; MON,  $\beta$ -myrcene, Z- $\beta$ -ocimene and E- $\beta$ -ocimene; NER, nerol and neral; PHE, 2-phenylethanol and phenylacetaldehyde; SES,  $\delta$ -cadinene, elemol,  $\alpha$ -cadinol,  $\tau$ -cadinol and  $\tau$ -muurolol; TMB, 1,3,5-trimethoxybenzene.

### Dataset S3

List of ESTs with homologies to NUDX proteins in the rose transcriptome database (15). ESTs in bold correspond to *RhNUDX1*. Values represent *in silico* expression analyses of selected transcripts in fully opened flowers library (relative RPKM counts, (45)).

## References and Notes

1. A. Vainstein, E. Lewinsohn, E. Pichersky, D. Weiss, Floral fragrance. New inroads into an old commodity. *Plant Physiol.* **127**, 1383–1389 (2001). [Medline](#) [doi:10.1104/pp.010706](#)
2. A. M. Borda, D. G. Clark, D. J. Huber, B. A. Welt, T. A. Nell, Effects of ethylene on volatile emission and fragrance in cut roses: The relationship between fragrance and vase life. *Postharvest Biol. Technol.* **59**, 245–252 (2011). [doi:10.1016/j.postharvbio.2010.09.008](#)
3. A. Joichi, K. Yomogida, K.-I. Awano, Y. Ueda, Volatile components of tea-scented modern roses and ancient Chinese roses. *Flavour Fragrance J.* **20**, 152–157 (2005). [doi:10.1002/ffj.1388](#)
4. G. Scalliet, F. Piola, C. J. Douady, S. Réty, O. Raymond, S. Baudino, K. Bordji, M. Bendahmane, C. Dumas, J. M. Cock, P. Hugueney, Scent evolution in Chinese roses. *Proc. Natl. Acad. Sci. U.S.A.* **105**, 5927–5932 (2008). [Medline](#) [doi:10.1073/pnas.0711551105](#)
5. Y. Kaminaga, J. Schnepf, G. Peel, C. M. Kish, G. Ben-Nissan, D. Weiss, I. Orlova, O. Lavie, D. Rhodes, K. Wood, D. M. Porterfield, A. J. Cooper, J. V. Schloss, E. Pichersky, A. Vainstein, N. Dudareva, Plant phenylacetaldehyde synthase is a bifunctional homotetrameric enzyme that catalyzes phenylalanine decarboxylation and oxidation. *J. Biol. Chem.* **281**, 23357–23366 (2006). [Medline](#) [doi:10.1074/jbc.M602708200](#)
6. I. Guterman, M. Shalit, N. Menda, D. Piestun, M. Dafny-Yelin, G. Shalev, E. Bar, O. Davydov, M. Ovadis, M. Emanuel, J. Wang, Z. Adam, E. Pichersky, E. Lewinsohn, D. Zamir, A. Vainstein, D. Weiss, Rose scent: Genomics approach to discovering novel floral fragrance-related genes. *Plant Cell* **14**, 2325–2338 (2002). [Medline](#) [doi:10.1105/tpc.005207](#)
7. M. Rodríguez-Concepción, A. Boronat, Elucidation of the methylerythritol phosphate pathway for isoprenoid biosynthesis in bacteria and plastids. A metabolic milestone achieved through genomics. *Plant Physiol.* **130**, 1079–1089 (2002). [Medline](#) [doi:10.1104/pp.007138](#)
8. F. Chen, D. Tholl, J. Bohlmann, E. Pichersky, The family of terpene synthases in plants: A mid-size family of genes for specialized metabolism that is highly diversified throughout the kingdom. *Plant J.* **66**, 212–229 (2011). [Medline](#) [doi:10.1111/j.1365-313X.2011.04520.x](#)
9. Y. Iijima, D. R. Gang, E. Fridman, E. Lewinsohn, E. Pichersky, Characterization of geraniol synthase from the peltate glands of sweet basil. *Plant Physiol.* **134**, 370–379 (2004). [Medline](#) [doi:10.1104/pp.103.032946](#)
10. M. J. Bessman, D. N. Frick, S. F. O’Handley, The MutT proteins or “Nudix” hydrolases, a family of versatile, widely distributed, “housecleaning” enzymes. *J. Biol. Chem.* **271**, 25059–25062 (1996). [Medline](#) [doi:10.1074/jbc.271.41.25059](#)
11. A. G. McLennan, The Nudix hydrolase superfamily. *Cell. Mol. Life Sci.* **63**, 123–143 (2006). [Medline](#) [doi:10.1007/s00018-005-5386-7](#)
12. E. Kraszewska, The plant Nudix hydrolase family. *Acta Biochim. Pol.* **55**, 663–671 (2008). [Medline](#)

13. K. Yoshimura, S. Shigeoka, Versatile physiological functions of the Nudix hydrolase family in *Arabidopsis*. *Biosci. Biotechnol. Biochem.* **79**, 354–366 (2015). [Medline](#)
14. H. Maki, M. Sekiguchi, MutT protein specifically hydrolyses a potent mutagenic substrate for DNA synthesis. *Nature* **355**, 273–275 (1992). [Medline](#) [doi:10.1038/355273a0](https://doi.org/10.1038/355273a0)
15. A. Dubois, S. Carrere, O. Raymond, B. Povreau, L. Cottret, A. Roccia, J.-P. Onesto, S. Sakr, R. Atanassova, S. Baudino, F. Foucher, M. Le Bris, J. Gouzy, M. Bendahmane, Transcriptome database resource and gene expression atlas for the rose. *BMC Genomics* **13**, 638–648 (2012). [Medline](#) [doi:10.1186/1471-2164-13-638](https://doi.org/10.1186/1471-2164-13-638)
16. V. Bergougnoux, J. C. Caillard, F. Jullien, J. L. Magnard, G. Scalliet, J. M. Cock, P. Hugueney, S. Baudino, Both the adaxial and abaxial epidermal layers of the rose petal emit volatile scent compounds. *Planta* **226**, 853–866 (2007). [Medline](#) [doi:10.1007/s00425-007-0531-1](https://doi.org/10.1007/s00425-007-0531-1)
17. O. Emanuelsson, H. Nielsen, S. Brunak, G. von Heijne, Predicting subcellular localization of proteins based on their N-terminal amino acid sequence. *J. Mol. Biol.* **300**, 1005–1016 (2000). [Medline](#) [doi:10.1006/jmbi.2000.3903](https://doi.org/10.1006/jmbi.2000.3903)
18. Y. Shang, K. E. Schwinn, M. J. Bennett, D. A. Hunter, T. L. Waugh, N. N. Pathirana, D. A. Brummell, P. E. Jameson, K. M. Davies, Methods for transient assay of gene function in floral tissues. *Plant Methods* **3**, 1–12 (2007). [Medline](#) [doi:10.1186/1746-4811-3-1](https://doi.org/10.1186/1746-4811-3-1)
19. P. J. Dunphy, Location and biosynthesis of monoterpenyl fatty acyl esters in rose petals. *Phytochemistry* **67**, 1110–1119 (2006). [Medline](#) [doi:10.1016/j.phytochem.2006.03.023](https://doi.org/10.1016/j.phytochem.2006.03.023)
20. M. J. O. Francis, M. O'Connell, The incorporation of mevalonic acid into rose petal monoterpenes. *Phytochemistry* **8**, 1705–1708 (1969). [doi:10.1016/S0031-9422\(00\)85957-9](https://doi.org/10.1016/S0031-9422(00)85957-9)
21. D. Hampel, A. Mosandl, M. Wüst, Biosynthesis of mono- and sesquiterpenes in strawberry fruits and foliage: 2H labeling studies. *J. Agric. Food Chem.* **54**, 1473–1478 (2006). [Medline](#) [doi:10.1021/jf0523972](https://doi.org/10.1021/jf0523972)
22. D. Hampel, A. Swatski, A. Mosandl, M. Wüst, Biosynthesis of monoterpenes and norisoprenoids in raspberry fruits (*Rubus idaeus* L.): The role of cytosolic mevalonate and plastidial methylerythritol phosphate pathway. *J. Agric. Food Chem.* **55**, 9296–9304 (2007). [Medline](#) [doi:10.1021/jf071311x](https://doi.org/10.1021/jf071311x)
23. M. Gutensohn, I. Orlova, T. T. Nguyen, R. Davidovich-Rikanati, M. G. Ferruzzi, Y. Sitrit, E. Lewinsohn, E. Pichersky, N. Dudareva, Cytosolic monoterpene biosynthesis is supported by plastid-generated geranyl diphosphate substrate in transgenic tomato fruits. *Plant J.* **75**, 351–363 (2013). [Medline](#) [doi:10.1111/tpj.12212](https://doi.org/10.1111/tpj.12212)
24. S. Frick, R. Nagel, A. Schmidt, R. R. Bodemann, P. Rahfeld, G. Pauls, W. Brandt, J. Gershenzon, W. Boland, A. Burse, Metal ions control product specificity of isoprenyl diphosphate synthases in the insect terpenoid pathway. *Proc. Natl. Acad. Sci. U.S.A.* **110**, 4194–4199 (2013). [Medline](#) [doi:10.1073/pnas.1221489110](https://doi.org/10.1073/pnas.1221489110)
25. S. Gagnot, J. P. Tamby, M. L. Martin-Magniette, F. Bitton, L. Taconnat, S. Balzergue, S. Aubourg, J. P. Renou, A. Lecharny, V. Brunaud, CATdb: A public access to *Arabidopsis*

transcriptome data from the URGV-CATMA platform. *Nucleic Acids Res.* **36** (suppl. 1), D986–D990 (2008). [Medline doi:10.1093/nar/gkm757](#)

26. T. Barrett, D. B. Troup, S. E. Wilhite, P. Ledoux, D. Rudnev, C. Evangelista, I. F. Kim, A. Soboleva, M. Tomashevsky, R. Edgar, NCBI GEO: Mining tens of millions of expression profiles—database and tools update. *Nucleic Acids Res.* **35** (suppl. 1), D760–D765 (2007). [Medline doi:10.1093/nar/gkl887](#)
27. A. Dubois, A. Remay, O. Raymond, S. Balzergue, A. Chauvet, M. Maene, Y. Pécrix, S. H. Yang, J. Jeauffre, T. Thouroude, V. Boltz, M. L. Martin-Magniette, S. Janczarski, F. Legeai, J. P. Renou, P. Vergne, M. Le Bris, F. Foucher, M. Bendahmane, Genomic approach to study floral development genes in *Rosa* sp. *PLOS ONE* **6**, e28455–e28468 (2011). [Medline doi:10.1371/journal.pone.0028455](#)
28. J. Vandesompele, K. De Preter, F. Pattyn, B. Poppe, N. Van Roy, A. De Paepe, F. Speleman, Accurate normalization of real-time quantitative RT-PCR data by geometric averaging of multiple internal control genes. *Genome Biol.* **3**, research0034.1–research0034.12 (2002). [Medline doi:10.1186/gb-2002-3-7-research0034](#)
29. T. Thiel, R. Kota, I. Grosse, N. Stein, A. Graner, SNP2CAPS: A SNP and INDEL analysis tool for CAPS marker development. *Nucleic Acids Res.* **32**, e5 (2004). [Medline doi:10.1093/nar/gnh006](#)
30. J. W. Van Ooijen, JoinMap 4, Software for the calculation of genetic linkage maps in experimental populations (Kyazma, Wageningen, Netherlands, 2006).
31. L. Hibrand-Saint Oyant, L. Crespel, S. Rajapakse, L. Zhang, F. Foucher, Genetic linkage maps of rose constructed with new microsatellite markers and locating QTL controlling flowering traits. *Tree Genet. Genomes* **4**, 11–23 (2008). [doi:10.1007/s11295-007-0084-2](#)
32. M. Spiller, M. Linde, L. Hibrand-Saint Oyant, C. J. Tsai, D. H. Byrne, M. J. Smulders, F. Foucher, T. Debener, Towards a unified genetic map for diploid roses. *Theor. Appl. Genet.* **122**, 489–500 (2011). [Medline doi:10.1007/s00122-010-1463-x](#)
33. J. W. Van Ooijen, MapQTL 5, Software for the mapping of quantitative trait loci in experimental populations (Kyazma, Wageningen, Netherlands, 2004).
34. G. A. Churchill, R. W. Doerge, Empirical threshold values for quantitative trait mapping. *Genetics* **138**, 963–971 (1994). [Medline](#)
35. H. Batoko, H.-Q. Zheng, C. Hawes, I. Moore, A rab1 GTPase is required for transport between the endoplasmic reticulum and golgi apparatus and for normal golgi movement in plants. *Plant Cell* **12**, 2201–2218 (2000). [Medline doi:10.1105/tpc.12.11.2201](#)
36. M. D. Curtis, U. Grossniklaus, A gateway cloning vector set for high-throughput functional analysis of genes in planta. *Plant Physiol.* **133**, 462–469 (2003). [Medline doi:10.1104/pp.103.027979](#)
37. M. Karimi, D. Inzé, A. Depicker, GATEWAY vectors for *Agrobacterium*-mediated plant transformation. *Trends Plant Sci.* **7**, 193–195 (2002). [Medline doi:10.1016/S1360-1385\(02\)02251-3](#)

38. P. Vergne, M. Maene, G. Gabant, A. Chauvet, T. Debener, M. Bendahmane, Somatic embryogenesis and transformation of the diploid *Rosa chinensis* cv Old Blush. *Plant Cell Tissue Organ Cult.* **100**, 73–81 (2010). [doi:10.1007/s11240-009-9621-z](https://doi.org/10.1007/s11240-009-9621-z)
39. D. Busso, B. Delagoutte-Busso, D. Moras, Construction of a set Gateway-based destination vectors for high-throughput cloning and expression screening in *Escherichia coli*. *Anal. Biochem.* **343**, 313–321 (2005). [Medline](#) [doi:10.1016/j.ab.2005.05.015](https://doi.org/10.1016/j.ab.2005.05.015)
40. G. Scalliet, C. Lionnet, M. Le Bechec, L. Dutron, J. L. Magnard, S. Baudino, V. Bergougoux, F. Jullien, P. Chambrier, P. Vergne, C. Dumas, J. M. Cock, P. Hugueney, Role of petal-specific orcinol O-methyltransferases in the evolution of rose scent. *Plant Physiol.* **140**, 18–29 (2006). [Medline](#) [doi:10.1104/pp.105.070961](https://doi.org/10.1104/pp.105.070961)
41. J. D. Bendtsen, H. Nielsen, G. von Heijne, S. Brunak, Improved prediction of signal peptides: SignalP 3.0. *J. Mol. Biol.* **340**, 783–795 (2004). [Medline](#) [doi:10.1016/j.jmb.2004.05.028](https://doi.org/10.1016/j.jmb.2004.05.028)
42. T. Ogawa, K. Yoshimura, H. Miyake, K. Ishikawa, D. Ito, N. Tanabe, S. Shigeoka, Molecular characterization of organelle-type Nudix hydrolases in *Arabidopsis*. *Plant Physiol.* **148**, 1412–1424 (2008). [Medline](#) [doi:10.1104/pp.108.128413](https://doi.org/10.1104/pp.108.128413)
43. D. Gunawardana, V. A. Likic, K. R. Gayler, A comprehensive bioinformatics analysis of the Nudix superfamily in *Arabidopsis thaliana*. *Comp. Funct. Genomics* **2009**, 820381 (2009). [Medline](#) [doi:10.1155/2009/820381](https://doi.org/10.1155/2009/820381)
44. S. Götz, J. M. García-Gómez, J. Terol, T. D. Williams, S. H. Nagaraj, M. J. Nueda, M. Robles, M. Talón, J. Dopazo, A. Conesa, High-throughput functional annotation and data mining with the Blast2GO suite. *Nucleic Acids Res.* **36**, 3420–3435 (2008). [Medline](#) [doi:10.1093/nar/gkn176](https://doi.org/10.1093/nar/gkn176)
45. A. Mortazavi, B. A. Williams, K. McCue, L. Schaeffer, B. Wold, Mapping and quantifying mammalian transcriptomes by RNA-Seq. *Nat. Methods* **5**, 621–628 (2008). [Medline](#) [doi:10.1038/nmeth.1226](https://doi.org/10.1038/nmeth.1226)